Montogue

Quiz HT110

COMBUSTION Engineering

Lucas Monteiro Nogueira

PROBLEMS

Problem 1

A laminar flame propagates through a combustible mixture in a horizontal tube 3 cm in diameter. The tube is open at both ends. Due to buoyancy effects, the flame tilts at a 45° angle to the normal and is planar. Assume the tilt is a straight flame front. The normal laminar flame speed for the combustible mixture is 40 cm/s. If the unburned gas mixture has a density of 0.0015 g/cm^3, what is the mass burning rate of the mixture in grams per second under this laminar flow condition?

A) Mass flow rate = 0.3 g/s
B) Mass flow rate = 0.6 g/s
C) Mass flow rate = 1.2 g/s
D) Mass flow rate = 1.8 g/s

Problem 2

Evaluate the following statements.

1.( ) A laminar butane jet flame burning in air has pressure of 1 atm and fuel temperature of 350 K. The mass flow rate of fuel is 3.5×10^{-6} kg/s and the density of butane in the conditions at hand is 1.8 kg/m^3. The flame temperature is taken as 2500 K and the mass diffusivity is 2.5×10^{-5} m^2/s. Using the semi-empirical equation 1.1 in the Additional Information section, we can establish that the flame height of the laminar flame in question is greater than 7 centimeters.

2.( ) A methanol non-premixed free jet is used as a pilot flame in a furnace. The flame height is 7 cm, the fire temperature is 2500 K, and the quiescent air surrounding the flame has temperature equal to 298 K and pressure equal to 1 atm. Assume the fuel temperature is identical to the temperature of the quiescent medium. The mass diffusivity is 1.2×10^{-5} m^2/s. Using semi-empirical equation 1.1 in the Additional Information section, we can surmise that the heat release rate of this laminar flame is greater than 125 W. Assume the lower heating value of methanol to be 20 kJ/g.

Problem 3

Calculate the Damköhler number for a turbulent flame described by the following characteristics:

Integral length = 1/4 of the domain length
Laminar flame thickness = 0.08 mm
Mean velocity = 2 m/s
Turbulent intensity = 10%
Laminar burning velocity = 0.8 m/s
Domain length = 1 m

A) *Da* = 625
B) *Da* = 1250
C) *Da* = 12,500
D) *Da* = 18,000

▶ Problem 4

For the two-dimensional problem of a pair of parallel plates, the quenching distance of a flame can be defined as the distance between the plates such that the rate of heat generation is exactly equal to the rate of heat removal. Assume a system of two parallel plates separated by a distance equal to the quenching distance d_q. Between the plates is a hydrocarbon flame burning at 2200 K, starting at a temperature of 300 K. The thermal conductivity and specific heat capacity of the gas that feeds the flame are 0.09 W/m·K and 2.23 kJ/kg·K, respectively; the lowest temperature at which the flame can propagate is 450 K. The stoichiometric mole fraction of the combustible mixture is 1.4 and the reaction rate is 1.2 g/s·m^3. Compute the quenching distance for this system.

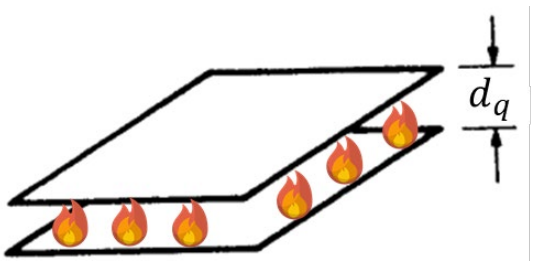

A) d_q = 3.0 cm
B) d_q = 5.2 cm
C) d_q = 8.7 cm
D) d_q = 11.0 cm

▶ Problem 5

Regarding the theory of combustion, true or false?

1.( ) In the framework of the Zel'dovich-Frank-Kamentskii theory of flame propagation, it can be shown that the normal flame velocity of a bimolecular reaction is independent of pressure.

2.( ) Despite its inherent simplicity, the Burke-Schumann diffusion flame model has been shown to offer a reasonably accurate representation of the flame height of an underventilated flame. The B-S flame is reasonably accurate because it does not involve drastic assumptions about the process being modelled; indeed, Burke and Schumann added realism to their approach by considering both radial and axial mass diffusion.

3.( ) An ethane cylinder containing 1 kg of gas is leaking into a 3.5 m × 4.5 m × 2.5 m room at 25°C and 1 atm. After a long time, the fuel gas and room air are well mixed. We can surmise that the mixture in the room is flammable. To evaluate this statement, bear in mind that ethane has a lean flammability limit of 0.50 and a rich flammability limit of 2.72; also, the stoichiometric mass air-fuel ratio for ethane is 16.0.

4.( ) The following graph shows the adiabatic flame temperature for a stoichiometric CH_4 flame as a function of the volumetric content of O_2 in the oxidizing mixture. With reference to this graph, we see that a methane flame with 40% oxygen will have an adiabatic flame temperature greater than 2500°C.

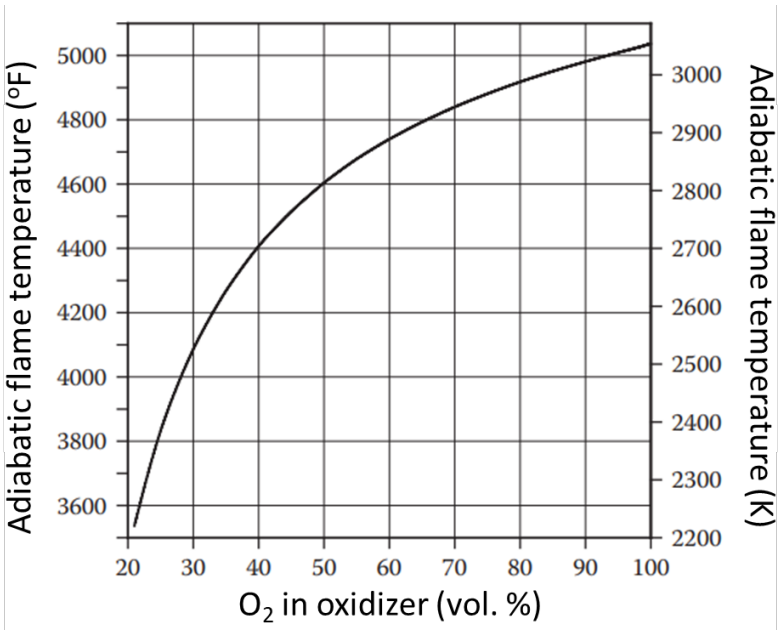

5.( ) The following graph shows experimentally derived quenching distances for a propane flame as functions of the volumetric oxygen proportion in the $O_2 + N_2$ oxidant mixture. As can be seen, increasing the proportion of gaseous oxygen in the oxidant mixture allows for a more stable flame.

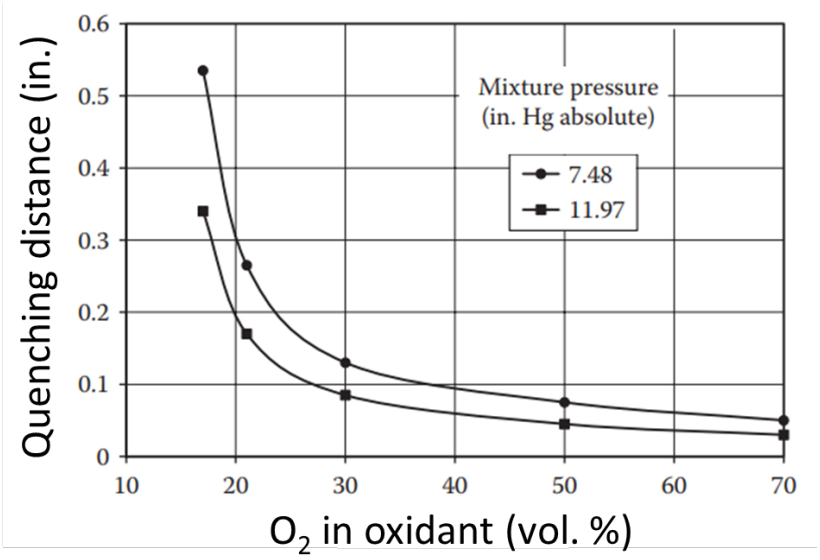

Dowdy *et al.* (1991) devised a technique for determining burning velocities and stretch effects in expanding hydrogen-air spherical flames at constant pressure. The following figure shows the burning velocities obtained by those workers as a function of stoichiometry. The points indicate experimental results, whereas the solid line is a polynomial fit to the experimental data; the agreement is clearly excellent.

6.( ) The graph indicates that a 1:1 stoichiometric hydrogen-air fire has burning velocity greater than 2.5 m/s. ■ **(A black square indicates the end of a multi-paragraph statement.)**

Recommended research: Dowdy *et al.* (1991).

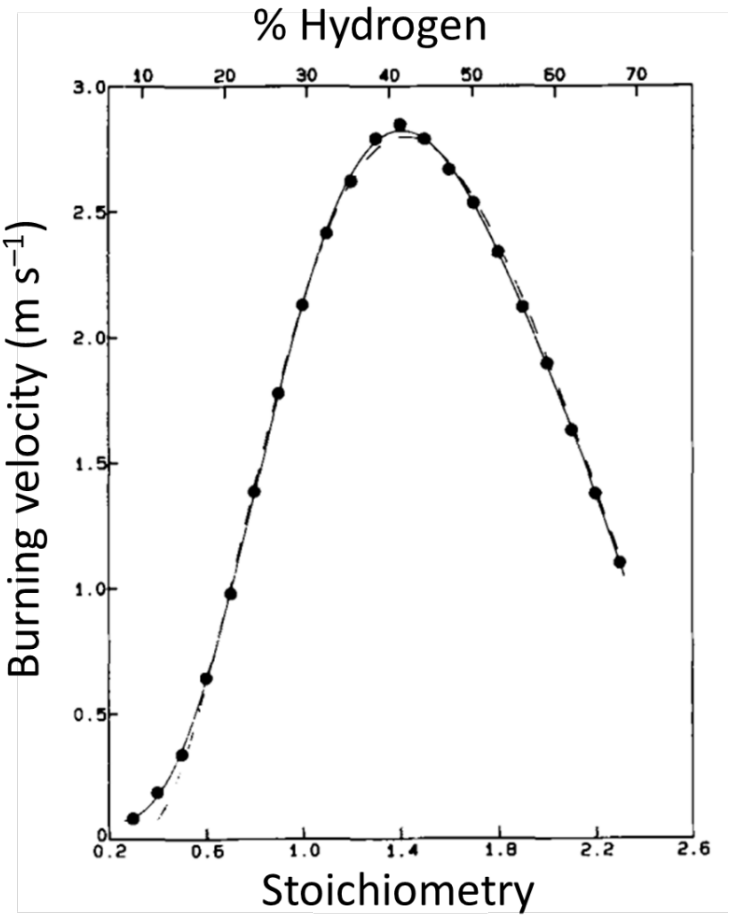

7.( ) A 1.6-mm diameter circular nozzle is discharging methane into the ambient air. The methane and air are both at 20°C, for which the densities of the two gases may be taken as 0.668 and 1.205 kg/m^3, respectively. We may conclude that the air-to-fuel ratio at a distance of 20 cm from the nozzle exit is greater than 50.

8.( ) The following chart shows the maximum flame velocity for the three main hydrocarbon families as a function of the number of carbon atoms. The plot indicates that the maximum flame velocity of alkanes is largely independent of the number of carbons.

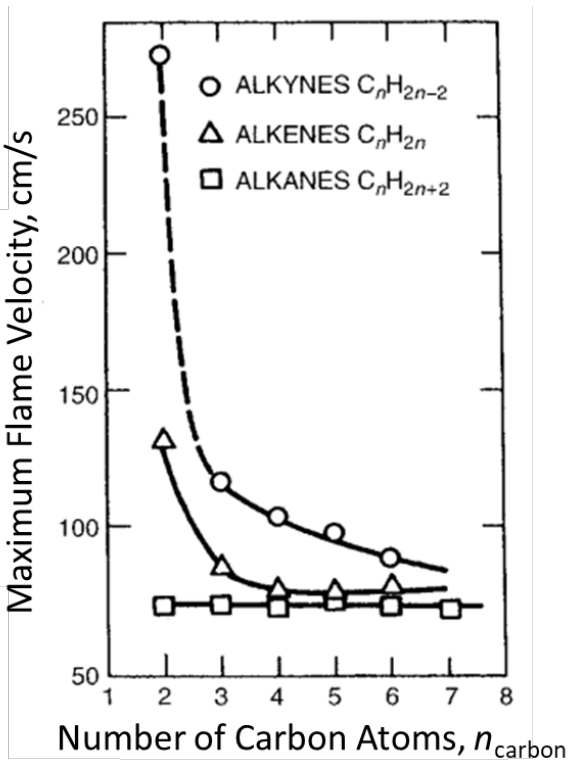

9.( ) A jet of acetylene (C_2H_2) exits a 20-mm diameter nozzle into still air at 67°C and 1 atm. We can surmise that the spreading angle of a jet with velocity equal to 4 cm/s is more than 3 times greater than the spreading angle of a jet with velocity equal to 20 cm/s. The viscosity of acetylene at the temperature of interest can be taken as 9.5×10^{-5} Pa·s.

10.( ) Reconsider the 20-cm/s jet introduced in the previous statement. With the properties specified in that statement, we may conclude that the jet centerline mass fraction will reduce to the stoichiometric value at an axial distance greater than 1.4 m away from the exit.

11.( ) The flame speed of a combustible hydrocarbon-air mixture is known to be 30 cm/s. The activation energy of such hydrocarbon flame reactions is generally assumed to be 160 kJ/mol. The true adiabatic flame temperature for this mixture is known to be 1600 K. An inert diluent is added to the mixture to lower the flame temperature to 1450 K. Since the reaction is of second-order, the addition of the inert can be considered to have no other effect on any property of the system. Accordingly, we can surmise that the flame speed *after* the diluent is added is greater than 20 cm/s.

12.( ) A drapery made of cotton has density 1.3 g/cm^3, specific heat capacity 0.34 cal/g·K, and thickness 1.5 mm. Assuming the ignition temperature is 300°C and the material, which is initially at 0°C, is subjected to a radiant heat flux of 30 kW/m^2, we can surmise that the drapery will ignite within more than 6 seconds.

13.( ) A 2-cm thick plywood board is subjected to a heat flux of 40 kW/m^2. Assuming that the plywood has ignition temperature equal to 325°C, thermal conductivity 0.16 W/m·K, density 800 kg/m^3, and specific heat capacity 2.8 kJ/kg·K, we can surmise that the board will ignite within more than 21 seconds. Assume the ambient temperature to be 0°C.

14.( ) Considering a 1.4-m diameter pool fire of gasoline, for which we may take a burning mass flux of 55 g/m^2·s and a heat of combustion of 43.7 kJ/g, the flame height can be calculated to be greater than 5 meters. In your analysis of this statement, use the Heskestad formula (equation 6).

15.( ) A pool fire fueled by heptane was observed to have a diameter of 0.8 m and a flame height of 3 m. The heat of combustion of heptane can be taken as 44.6 kJ/g. We conclude that the fuel mass flux that sustains this pool fire is greater than 42 g/m^2·s.

In the so-called polygeneration coal system, syngas is used as the fuel to generate electricity. Syngas fuels are primarily composed of H_2 and CO, but may also contain N_2, CO_2, H_2O, CH_4, and other higher-order hydrocarbons. Dong *et al.* (2009) used a Bunsen burner arrangement to produce correlations for the laminar flame speed of H_2/CO flames. They first noted that, for a H_2/air mixture, the laminar flame speed (m/s) for an equivalence ratio ϕ of H_2 varies according to

$$S_{\mathrm{H_2}} = 0.08925 + 1.59163\phi - 0.91917\phi^2 + 0.52964\phi^3 \; ; \left(\phi \in \left(0.7, 2.1\right)\right)$$

Similarly, the laminar flame speed (also in m/s) for a CO/air flame varies with the equivalence ratio ϕ of CO according to

$$S_{\mathrm{CO}} = 0.03276 + 0.18198\phi - 0.04156\phi^2 - 0.00791\phi^3 \; ; \left(\phi \in \left(0.7, 2.1\right)\right)$$

Lastly, in order to calculate the laminar flame speed for a H_2/CO mixture, we define $(S_x - S_{CO})/(S_{H_2} - S_{CO})$ as the laminar flame speed increment, where S_x is the laminar flame speed for a H_2/CO mixture containing *x*% of H_2. The laminar flame speed increment is related to the fraction of H_2 by the linear fit

$$\frac{S_x - S_{\mathrm{CO}}}{S_{\mathrm{H_2}} - S_{\mathrm{CO}}} = -0.05914 + 0.00875x$$

16.( ) Equipped with these expressions, we surmise that a H_2/CO flame with 40% hydrogen content, based on H_2/air and CO/air mixtures with equivalence ratio equal to 1.0, will be greater than 2 m/s. ■

Recommended research: Dong *et al.* (2009).

It is well-documented that most realistic flames are subjected to stretch due to either flow nonuniformity, flame curvature, or flame acceleration. It is then of interest to establish how flame speeds can be affected by stretch. This problem was tackled by Wu and Law (1985), who showed that laminar flame speed varies linearly with stretch rate, which they denoted as Γ; accordingly, the laminar flame velocity can be established with a speed versus stretch plot, by linearly extrapolating the value of S_L for stretched flames to vanishing stretch rate (i.e., $\Gamma = 0$) and reading the vertical intercept.

17.( ) Wu and his colleague showed that, under the proper conditions, this technique is valid even for highly diffusive systems such as the H_2-air flame, for which the influence of stretch is particularly pronounced. ■

Recommended research: Wu and Law (1985).

18.( ) Reconsider the Wu and Law (1985) paper mentioned in the previous statement. Other extrapolation methods used to relate stretch and laminar flame speed have been introduced in the years since – including, for instance, Kelley and Law (2009) – and the uncertainty associated with some of these approaches was closely examined by Wu *et al.* (2014). Wu *et al.* (2014) found that extrapolation methods can yield very inaccurate results; inaccuracies were found to be greater for H_2-air flames than for *n*-heptane-air flames at the same equivalence ratio.

Recommended research: Kelley and Law (2009); Wu *et al.* (2014).

Counterflow twin-flames (CTFs) (i.e., configurations in which two identical, nozzle-generated flows of the combustible mixture of interest are impinged onto each other) have also been used in the determination of laminar flame speed. In a 'classic' determination of S_L via CTF, the flow field is mapped with laser Doppler velocimetry, the minimum in the velocity profile is identified as the reference upstream burning velocity, $S_{u,ref}$, and the velocity gradient ahead of the minimum point is taken as the strain rate, K. $S_{u,ref}$ is plotted for various K and, assuming that $S_{u,ref}$ varies linearly with K, linear extrapolation to $K = 0$ yields the desired laminar flame speed.

19.( ) Vagelopoulos *et al.* (1994) investigated experimental parameters that may affect laminar flame speed measurements with CTFs, and found that the linear extrapolation approach is more accurate for high Karlovitz numbers (Ka of the order of 1.0 is optimal) and small nozzle separation distances. ■

Recommended research: Vagelopoulos *et al.* (1994).

20.( ) There is some debate on the distance required for a hydrogen-oxygen flame front propagating in a cylindrical tube to undergo a deflagration-to-detonation transition; this distance is sometimes known as the *run-up distance*. Some workers have indicated that run-up distance may increase with tube diameter. Indeed, Kuznetsov (2005) found that the run-up distance in a hydrogen-oxygen mixture in a smooth cylindrical tube is proportional to tube diameter but bears no relation to the scale of turbulent pulsations observed in the system.

Recommended research: Kuznetsov *et al.* (2005).

Yu *et al.* (1986) used the symmetric counterflow flame to measure the laminar flame speeds for methane-air and propane-air mixtures with hydrogen addition, and found that, regardless of whether the mixture was lean or rich, flame speeds increased linearly with a hydrogen addition parameter R_H.

Decades later, Tang *et al.* (2011) set about proposing a mechanistic interpretation for this linear relationship. They noted that the laminar burning flux f, which is the density-weighted flame speed and functions as the eigenvalue for flame propagation, can be described by the proportion

$$f^2 \propto \mathrm{Le} \times \exp\left(-E_a \big/ R^0 T_{ad}\right)$$

where Le is the Lewis number, E_a is the activation energy, R^0 is the gas constant, and T_{ad} is the adiabatic flame temperature. Le, E_a, and T_{ad} can be considered representative of diffusional, kinetic, and thermal effects, respectively.

21.( ) Tang's sensitivity analysis for these three effects revealed that the linear relation in question is substantially related to the kinetic and thermal contributions, but only marginally affected by diffusional effects. ■

Recommended research: Yu *et al.* (1986); Tang *et al.* (2011).

Laminar flame width is a loosely defined concept, as investigators have used the phrase over the years to define different characteristic lengths of fire phenomena. Blint (1986) summarized some definitions for flame width. For example, in a one-zone fire model, we may use a flame width δ_T which depends on the shape of the temperature profile according to

$$\delta_T = \left(T_a - T_u\right) \Big/ \left(\frac{dT}{dx}\right)_{\max}$$

where T_a is the adiabatic flame temperature, T_u is the unburned gas temperature, and $(dT/dx)_{\max}$ is the temperature gradient at the inflection point.

In two-zone flame models the first zone has diffusion and convection dominating and the second has heat release dominating. In such a case, the characteristic length is determined by balancing the rate of heat production in the second zone with the rate with which it is conducted away into the first zone. One definition in this case is

$$\delta_Q = \text{Half-width at half max. of the heat release zone}$$

Although δ_Q is a characteristic of the flame which will affect the shape of the temperature profile, it is not measurable and must be extracted from the temperature profile using a reaction mechanism.

Alternatively, a flame width can be defined as the product between a characteristic reaction time τ and the laminar flame speed,

$$\delta_\tau = \tau \times S_u$$

22.( ) Blint (1986) used a simple model and detailed data on transport properties of burned and unburned gases to look for correlations between the flame widths δ_T, δ_Q, and δ_τ. One of his findings was that a flame width δ_Q based on the half-width of the heat release rate did not correlate well with any reasonable transport properties of the gases. ■

Recommended research: Blint (1986).

It is well known that hydrogen-air mixtures ignited in a standard gravitational field may yield near-stationary flames (i.e., flames that rise at constant speed) that do not act as ignition sources for the surrounding mixture – that is, they do not generate unsteady radially propagating flames. Accordingly, there must be a stabilizing mechanism capable of confining the combustion to a small volume, and buoyancy-generated convection has been implied as one such mechanism. It may plausibly be speculated that at zero gravity, in the absence of convection, the corresponding stationary configuration is spherically symmetric; that is, we may speak of 'stationary flame balls.'

23.( ) Indeed, theoretical analysis by Buckmaster *et al.* (1990) has indicated that stationary flame balls are more stable than stationary plane flames, in that, for not-too-low Lewis numbers – say, $Le = 0.3$ – flame balls may exist in the presence of heat losses much stronger than those required to extinguish plane flames. ■

Recommended research: Buckmaster *et al.* (1990).

24.( ) Smooke *et al.* (1989) conducted a detailed numerical analysis of an axisymmetric diffusion flame in which a cylindrical fuel stream is surrounded by a co-flowing oxidizer jet. Their model included a 42-reaction, 15-species-strong analysis, and at the time was one of the most advanced computational combustion studies ever produced. Its main strength, of course, was that it was based on a three-dimensional framework and dealt away with the use of stream functions.

Recommended research: Smooke *et al.* (1989).

25.( ) Zimont *et al.* (1998) introduced another noteworthy numerical study of combustion. Their model is based on a three-dimensional, finite-volume scheme that, unlike several contemporary approaches, relies on readily obtainable parameters, with no resort to the arcane inputs that plague several other turbulent combustion models. Their model was validated on the basis of experimental data for an ABB double cone burner (DCB) and reproduced flame dynamics remarkably well, including, for instance, a precise representation of the DCB's central recirculation zone.

Recommended research: Zimont *et al.* (1998).

26.( ) Barlow and Frank (1998) performed simultaneous measurements of species mass fractions of H_2O, CO_2, OH, CO, H_2 and NO in six piloted methane-air jet flames. Conditional probability density functions of each species were prepared, and significant changes were noted as the jet Reynolds number was increased from the laminar regime to increasingly turbulent settings. Specifically, Barlow and his colleague verified that, as the jets were made more turbulent, the peak mass fractions of OH, H_2, NO, H_2O, and CO_2 all increased, whereas that of CO decreased.

Recommended research: Barlow and Frank (1998).

Hawkes and Cant (2000) simulated turbulent premixed combustion using a flamelet approach based on the concept of filtered flame surface density (FSD), which is essentially the flame surface area per unit volume contained within the LES filtering volume. Their test geometry of choice was a rectangular box wherein a premixed flame entered through one inflow face and exited through the opposite face, as shown to the side. As in other LES schemes, one important issue is the independence of the results on the filter width Δ; with this question in mind, Hawkes and his colleague conducted simulations with varying filter sizes, and in each simulation the relative proportion of resolved and sub-grid kinetic energy at inflow was determined from the known energy spectrum. In each case, the flame was initialized from an approximate planar laminar solution with an initial thickness governed by the value of Δ.

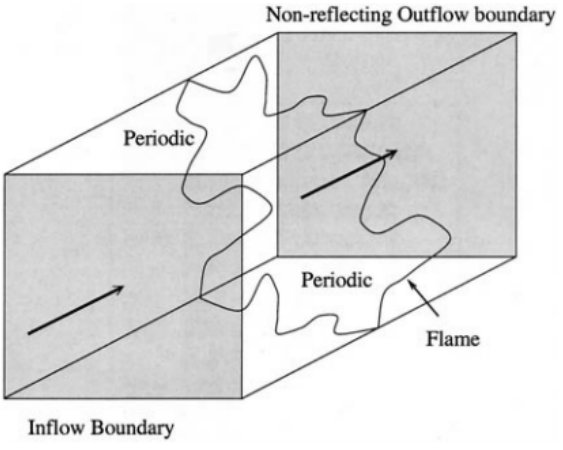

27.( ) The behavior of the simulations with respect to Δ showed worrisome results, notably the fact that, with increasing filter size, there was a decrease in flame thickness and an increase of resolved wrinkling, in direct contrast to what is expected of a LES-FSD numerical scheme. ■

Recommended research: Hawkes and Cant (2000).

28.( ) Bell *et al.* (2007) conducted an experimental study of a slot Bunsen flame fed by a stoichiometric methane-air mixture. Figure (a) below shows the instantaneous flame surface they obtained for the isotherm at 1684 K; the tiles marking the coflow are 0.5-cm squares. Figure (b), in turn, shows the probability density function they obtained for the flame curvature as determined from their experimental scheme (green line), 3D simulation (red line), and 2D simulation (blue line). In accordance with earlier observations by Ashurst and Shepherd (1998), Bell's simulation shows very substantial disagreement between 2D and 3D curvature computations.

Recommended research: Bell *et al.* (2007); Ashurst and Shepherd (1997).

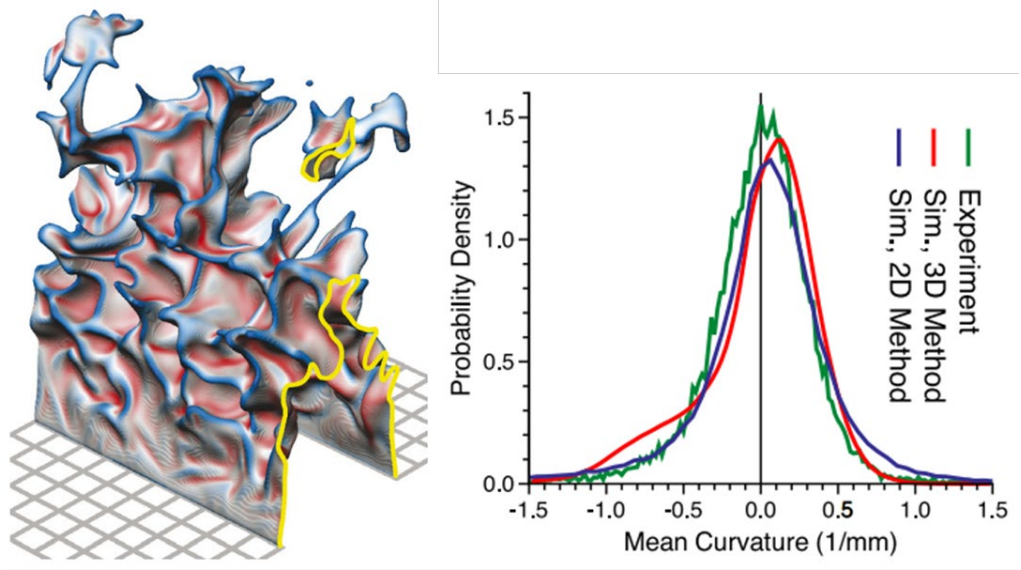

(a) **(b)**

29.( ) When a burner-stabilized jet flame is lifted from a burner by increasing the fuel or surrounding air co-flow velocity, the flame can stabilize without a physical element to use for stabilization, and a so-called lifted jet flame is created. Turbulent lifted jet flames have received substantial attention due to their importance in practical applications such as diesel engines. Of specific interest is the stabilization mechanism of a lifted-flame base, for which several hypotheses have been suggested. In one noteworthy study, Yoo *et al.* (2009), working with turbulent lifted hydrogen jet flames in heated coflow, found that auto-ignition is the likely stabilization mechanism of such flames. Their three-dimensional DNS simulations showed that perhydroxyl radical, HO_2, is important in initiating auto-ignition upstream of the flame base.

Recommended research: Yoo *et al.* (2009).

30.( ) Gruber *et al.* (2010) used direct numerical simulation (DNS) to study the dynamics of turbulent flame-wall interaction (FWI). Gruber's team studied a premixed, *v*-shaped hydrogen-air flame propagating in a plane channel, and reported several interesting findings on flow behavior in the vicinities of the wall. For instance, they found that flame thickness changed from a maximum thickness in the centerline to a gradually diminishing thickness towards the walls; the flame thickness just beside the wall was observed to be identical to the laminar flame thickness.

Recommended research: Gruber *et al.* (2010).

Use of Filter Density Functions (FDFs) in Large-Eddy Simulation (LES) and Probability Density Functions (PDFs) in Reynolds-Averaged Navier-Stokes (RANS) schemes are well-established means to help achieve closure in sub-grid scales of turbulent chemically reactive flows. In LES models, the most widely used FDF is the so-called β-function, which is a good *a priori* choice for several combustion problems, especially at high Reynolds numbers.

31.( ) However, the β-function does have appreciable shortcomings, most notably the facts that the presumption of a β-FDF has little theoretical basis, and, as noted by Tong (2001), conserved scalars used to model turbulent jet numerical schemes may involve bimodal behavior that a β-function cannot reliably represent. ■

Recommended research: Floyd *et al.* (2009); Tong (2001).

32.( ) A topic of active research is the interaction between flames and sound (pressure) waves. For example, sound propagation in a tube may modulate the inlet feeding rate of a fuel, causing equivalence ratio oscillations. Searby and Rochwerger (1991) found that a pressure oscillation of moderate level leads to parametric instability. However, it has likewise been shown that at sufficiently high amplitude, such disturbances may restabilize Darrieus-Landau instability and may even control the mean shape of a flame.

Recommended research: Searby and Rochwerger (1991); Wu *et al.* (2003).

Research indicates that the effect of a Darrieus-Landau disturbance depends on a flame's mixture-dependent length scale and this scale's relationship to the wavelength of the DL disturbance. This length scale, which is often several times greater than the flame thickness, suggests that larger flames may be subject to large-scale disturbance behavior not exhibited by flames constrained by smaller domains. Aiming to put these distinctions to the test, Lapenna *et al.* (2019) conducted direct numerical simulations (DNS) of two slot Bunsen flames, one representative of 'small-scale' flames and the other representative of 'large-scale' flames. The following figure shows the spatial distribution of the generalized flame surface density Σ for the small-scale slot flame, to the left, and for the large-scale slot flame, to the right; only half of the domain is shown in the x direction.

33.( ) Clearly, the density profiles indicate that the wrinkling factor is greater for the small-scale flame than for the large-scale one. ■

Recommended research: Lapenna *et al.* (2019).

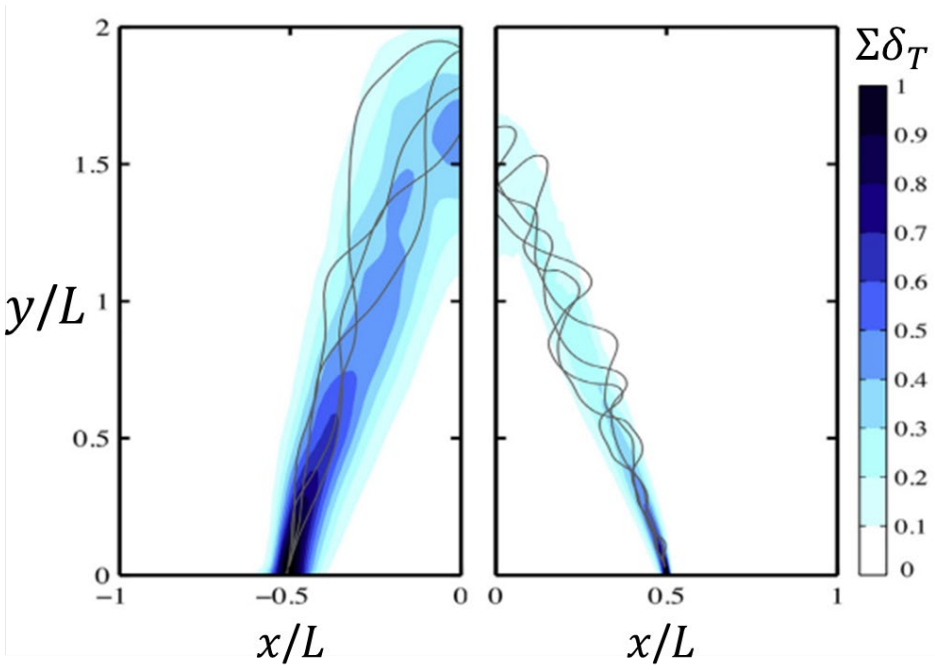

34.( ) Digital flame visualization techniques have evolved rapidly in recent years. One noteworthy contribution is Brisley *et al.* (2005), who were among the first to harness three-dimensional camera imaging in the visualization of gas-fired flames. Brisley's team opted for a single CCD camera system that could reconstruct typical flames and yield their temperature profiles. Importantly, Brisley's imaging scheme required flames to exhibit a high level of rotational symmetry, such that the flame appears to be identical when observed from different viewpoints around the burner axis. Since turbulent flames generally possess little to no rotational symmetry, Brisley's apparatus is not a viable choice for imaging turbulent flames.

Recommended research: Brisley *et al.* (2005).

35.( ) Chaudhuri *et al.* (2012) conducted experimental studies of constant-pressure expanding flames propagating in nearly homogeneous isotropic turbulence. Using the self-similar property of turbulent flame speeds, they showed that the turbulent flame speeds measured from the spherically expanding flames they investigated can be scaled by a single parameter, namely a turbulent Reynolds number based on the geometric and transport properties of the flame; no other dimensionless group was needed.

Recommended research: Chaudhuri *et al.* (2012).

36.( ) One interesting line of research concerns interactions between flames and electric fields. For example, Van den Boom *et al.* (2009) exposed laminar, flat, stoichiometric methane-air flames to an uniform DC electric field to investigate the effect on adiabatic burning velocity. Interestingly, van den Boom's team found that increasing the applied voltage led to deviations ΔS_L in burning velocity that increased linearly with the intensity of the applied voltage.

Recommended research: Van den Boom *et al.* (2009).

37.( ) Smoldering combustion has drawn the interest of the combustion community in recent years. One important contribution in the field is due to Bar-Ilan *et al.* (2004), who devised several experiments to study the effect of buoyancy on opposed smoldering (i.e., smoldering in which the flow of oxidizer is induced in the opposite direction of the propagation of the smolder front). Importantly, Bar-Ilan's team found that the oxidizer mass flux required to attain a given smolder velocity in normal gravity is lower than the mass flux needed to yield the same velocity in a microgravity environment.

Recommended research*:* Bar-Ilan *et al.* (2004).

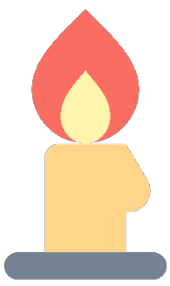

One of the simplest diffusion flame systems of practical interest is the paraffin candle. In spite of its apparently straightforward physics, a typical candle can exhibit very complex oscillatory dynamics, especially when several of them are positioned closely to one another.

38.( ) The oscillatory behavior of candle groups was studied by Chen *et al.* (2019), who showed, among other things, that when two candles are initially close and then gradually placed far apart, oscillatory behavior changes from incoherent oscillation at close distances, anti-phase oscillation at intermediate distances, and finally in-phase oscillation at large distances. ■

Recommended research*:* Chen *et al.* (2019).

▶ Problem 6

Lipatnikov and Chomiak (2002) revisited several experimental databases on turbulent flame speeds and proposed dimensionless-group correlations for each dataset. With reference to that paper, choose the alternative that matches the parameterization for a given database and the corresponding correlation for turbulent velocity U_t.

Recommended research*:* Lipatnikov and Chomiak (2002) and references therein.

Parameterization	Database
I. $U_t \propto u'(Ka)^{-0.31}$	**P.** Kobayashi *et al.* (1998)
II. $U_t \propto u'(Da)^{0.44}$	**Q.** Karpov and Severin (1978, 1980)
III. $U_f \propto u'(Da)^{0.37}(Re_t)^{0.04}$	**R.** Kido *et al.* (1989)
IV. $U_t \propto u'(Da)^{0.2}(Re_t)^{-0.3}$	**S.** Shy *et al.* (2000)
V. $U_t \propto u'(Ka)^{-0.41}$	**T.** Aldredge *et al.* (1998)

A) I.Q; II.R; III.S; IV.P; V.T;
B) I.S; II.Q; III.T; IV.P; V.R;
C) I.P; II.S; III.T; IV.Q; V.R;
D) I.R; II.S; III.P; IV.T; V.Q;
E) I.Q; II.R; III.P; IV.T; V.S;
F) I.S; II.R; III.P; IV.T; V.Q;

▶ Problem 7 (Modified from Flagan and Seinfeld, 1988)

Estimate the flame propagation velocity and flame thickness for stoichiometric combustion of premixed methane in air flowing in a 0.125-m diameter pipe with a cold gas velocity of 10 m/s. The initial pressure and temperature are 1 atm and 303 K, respectively. Take $\nu = 1.5\times10^{-5}$ m^2/s as the kinematic viscosity of methane. In the conditions at hand, the measured laminar flame speed for stoichiometric combustion of methane in air is about 0.38 m/s.

A) S_T = 0.85 m/s and δ_F = 2.92 mm
B) S_T = 0.85 m/s and δ_F = 5.84 mm
C) S_T = 1.70 m/s and δ_F = 2.92 mm
D) S_T = 1.70 m/s and δ_F = 5.84 mm

ADDITIONAL INFORMATION

Equations

Eq. 1.1 → *Roper's equation for flame length in a circular-port burner*

$$L_f = \frac{Q_F\left(T_\infty/T_F\right)}{4\pi D_\infty \ln\left(1+1/S\right)}\left(\frac{T_\infty}{T_f}\right)^{0.67}$$

where Q_F is fuel flow rate, S is the molar stoichiometric oxidizer-fuel ratio, D_∞ is a mean diffusion coefficient evaluated for the oxidizer at the oxidizer stream temperature T_∞, T_F is the fuel stream temperature, and T_f is the flame temperature.

Eq. 1.2 → *Correlation for flame length in a circular-port burner*

$$L_f = 1045\frac{Q_F\left(T_\infty/T_F\right)}{\left[\text{inverf}\left(\left(1+S\right)^{-1/2}\right)\right]^2}$$

where Q_F is fuel flow rate, S is the molar stoichiometric oxidizer-fuel ratio, T_∞ is the oxidizer stream temperature, and T_F is the fuel stream temperature. Quantities are in SI units.

Eq. 2.1 → *Roper's equation for flame length in a momentum-controlled slot burner*

$$L_f = \frac{b\beta^2 Q_F}{hID_\infty Y_{F,\text{stoic}}}\left(\frac{T_\infty}{T_F}\right)^2\left(\frac{T_f}{T_\infty}\right)^{0.33}$$

where b is the slot width, h is the slot height, $Y_{F,\text{stoic}}$ is the stoichiometric mass fraction of fuel, Q_F is fuel flow rate, D_∞ is a mean diffusion coefficient evaluated for the oxidizer at the oxidizer stream temperature T_∞, T_F is the fuel stream temperature, T_f is the flame temperature, I is the ratio of the actual initial momentum flow from the slot to that of uniform flow, and β is a coefficient that depends on the stoichiometric oxidizer-fuel ratio in accordance with

$$\beta = \frac{1}{4\,\text{inverf}\left[1/\left(1+S\right)\right]}$$

Eq. 2.2 → *Correlation for flame length in a momentum-controlled slot burner*

$$L_f = 86,400\frac{b\beta^2 Q_F}{hIY_{\text{F,stoic}}}\left(\frac{T_\infty}{T_F}\right)^2$$

where b is slot width, h is the slot height, $Y_{F,\text{stoic}}$ is the stoichiometric mass fraction of fuel, Q_F is fuel flow rate, I is the ratio of the actual initial momentum flow from the slot to that of uniform flow, T_∞ is the oxidizer fuel stream temperature, T_F is the fuel stream temperature, and β is identical to Eq. 2.1. Quantities are in SI units.

Eq. 3 → *Mass entrainment rate of a circular free jet*

$$\frac{\dot{m}_\infty}{\dot{m}_j} = 0.28\left(\frac{\rho_\infty}{\rho_j}\right)^{\frac{1}{2}}\left(\frac{x}{d}\right)$$

where $\dot{m}_\infty$ is the mass flow of the surrounding gas entrained, $\dot{m}_j$ is the mass flow of the jet, ρ_∞ is the density of the surrounding gas, ρ_j is the density of the free jet, x is the distance downstream of the nozzle exit, and d is the diameter of the nozzle port.

Eq. 4.1 → *Spreading angle of a jet*

$$\alpha = \tan^{-1}\left(2.97/\mathrm{Re}_{j,1}\right)$$

where α is the spreading angle and Re_j is the jet Reynolds number.

Eq. 4.2 → *Mass fraction of fuel in the centerline of a jet*

$$Y_{F,0} = 0.375\,\mathrm{Re}_j\left(\frac{x}{R}\right)^{-1}$$

where $Y_{F,0}$ is the mass fraction in the centerline of the jet, Re_j is the jet Reynolds number, R is the inlet entrance radius, and x is the axial distance from the jet entrance.

Eq. 5.1 → *Time to ignition for a thin object*

$$t_{\mathrm{ig}} = \frac{\rho c \ell\left(T_{\mathrm{ig}} - T_\infty\right)}{q_l''}$$

where t_{ig} is the time to ignition, ρ is the density of the object, ℓ is the thickness of the object, T_{ig} is the ignition temperature, T_∞ is the temperature of the surrounding medium, and q_l'' is the incident heat flux.

Eq. 5.2 → *Time to ignition for a thick object*

$$t_{\mathrm{ig}} = \frac{(\pi/4)k\rho c\left(T_{\mathrm{ig}} - T_\infty\right)^2}{q_l''^2}$$

where t_{ig} is the time to ignition, k is the thermal conductivity of the material, ρ is the density of the object, T_{ig} is the ignition temperature, T_∞ is the temperature of the surrounding medium, and q_l'' is the incident heat flux.

Eq. 6 → *Heskestad formula for height of flames from pool fires*

$$L_f = 0.23\dot{Q}^{2/5} - 1.02D$$

where $\dot{Q}$ is the combustion energy release rate in kW and D is the pool diameter in meters.

SOLUTIONS

P.1 ➡ ***Solution***

Firstly, the flame front area can be obtained by dividing the cross-sectional area of the tube by the cosine of the tilt angle,

$$A = \frac{\text{Tube cross-sectional area}}{\cos\left(\text{Tilt angle}\right)} = \frac{\frac{\pi}{4}\times 3^2}{\cos 45^\circ} = 10\,\mathrm{cm}^2$$

The mass burning rate is then

$$\text{Mass flow rate} = \rho A u = 0.0015\times 10\times 40 = \boxed{0.6\,\mathrm{g/s}}$$

▶ The correct answer is **B**.

P.2 ➡ ***Solution***

1.False. The expression to use is (equation 1.1)

$$L_f = \frac{Q_F\left(T_\infty/T_F\right)}{4\pi D_\infty \ln\left(1+1/S\right)}\left(\frac{T_\infty}{T_f}\right)^{0.67}$$

The molar stoichiometric fuel ratio S for a $C_\alpha H_\beta O_\gamma$ molecule burning with air is given by

$$S = 4.76\left(\alpha + \frac{\beta}{4} - \frac{\gamma}{2}\right)$$

For butane, $\alpha = 4$, $\beta = 10$, and $\gamma = 0$, so that

$$S = 4.76\left(4 + \frac{10}{4} - \frac{0}{2}\right) = 30.9$$

Next, the volumetric flow rate is obtained by dividing the mass flow by the specified density:

$$\dot{V}_{\text{fuel}} = \frac{3.5\times10^{-6}}{1.8} = 1.94\times10^{-6}\ \text{m}^3/\text{s}$$

Substituting into the equation for L_f, we obtain

$$L_f = \frac{\left(1.94\times10^{-6}\right)\times\left(350/350\right)}{4\pi\times\left(2.5\times10^{-5}\right)\times\ln\left(1+1/30.9\right)}\left(\frac{350}{2500}\right)^{0.67} = 0.0519\,\text{m}$$

$$\therefore \boxed{L_f = 5.19\,\text{cm}}$$

Note that we have assumed the fuel temperature T_F to be equal to the temperature T_∞ of the quiescent air. The flame height is close to 5 centimeters.

2.True. We first compute the molar stoichiometric fuel ratio, noting that, for methanol, we have $\alpha = 1$, $\beta = 4$, and $\gamma = 1$,

$$S = 4.76\left(\alpha + \frac{\beta}{4} - \frac{\gamma}{2}\right) = 4.76\times\left(1 + \frac{4}{4} - \frac{1}{2}\right) = 7.14$$

Next, we solve equation 1.1 for volumetric flow rate, giving

$$L_f = \frac{Q_F\left(T_\infty/T_F\right)}{4\pi D_\infty \ln\left(1+1/S\right)}\left(\frac{T_\infty}{T_f}\right)^{0.67} \rightarrow Q_F = \frac{L_f 4\pi D \ln\left(1+1/S\right)}{\left(T_\infty/T_F\right)\left(T_\infty/T_f\right)^{0.67}}$$

$$\therefore \dot{V}_{\text{fuel}} = \frac{7\times4\pi\times\left(1.2\times10^{-1}\right)\times\ln\left(1+1/7.14\right)}{\left(298/298\right)\times\left(298/2500\right)^{0.67}} = 5.75\,\text{cm}^3/\text{s}$$

$$\therefore \dot{V}_{\text{fuel}} = 5.75\times10^{-3}\ \text{L/s}$$

We proceed to compute the molar volume,

$$\frac{\text{Volume}}{n} = \frac{R_u T}{P} = \frac{0.0821\times298}{1.0} = 24.5\,\text{L/mol}$$

Then, the mass flow rate of the jet flame is

$$\dot{m}_{\text{fuel}} = \frac{\dot{V}_{\text{fuel}}}{24.5}\times M_{CH_3OH} = \frac{5.75\times10^{-3}}{24.5}\times32 = 0.00751\ \text{g/s}$$

The last step, noting that the LHV of methanol equals 20 kJ/g, is to compute the heat release rate,

$$LHV\times\dot{m}_{\text{fuel}} = 20{,}000\frac{\text{J}}{\cancel{\text{g}}}\times0.00751\frac{\cancel{\text{g}}}{\text{s}} = \boxed{150\,\text{W}}$$

P.3 ➡ *Solution*

Firstly, the characteristic flow time τ_{flow} is given by dividing the integral length scale by the turbulent velocity,

$$\tau_{\text{flow}} = \frac{\text{Integral length scale}}{\text{Turbulent velocity}}$$

The ILS was specified to be ¼ of the domain length, that is, ¼ × 1 = 0.25 m. The turbulent velocity, in turn, is obtained by multiplying the turbulent intensity (= 10%) by the mean velocity (= 2 m/s),

$$\text{Turbulent velocity} = 0.1 \times 2 = 0.2\,\text{m/s}$$

so that

$$\tau_{\text{flow}} = \frac{0.25}{0.2} = 1.25\,\text{s}$$

Similarly, the chemical time scale is obtained if we divide the laminar flame thickness by the laminar burning velocity,

$$\tau_{\text{chem}} = \frac{\text{Laminar flame thickness}}{\text{Laminar burning velocity}} = \frac{0.08 \times 10^{-3}}{0.8} = 10^{-4}\,\text{s}$$

Finally, the Damköhler number is calculated to be

$$\text{Da} = \frac{\tau_{\text{flow}}}{\tau_{\text{chem}}} = \frac{1.25}{10^{-4}} = \boxed{12,500}$$

▶ The correct answer is **C**.

P.4 ➡ ***Solution***

The rate of heat generation can be expressed as

$$\dot{q}_R = \phi_0 \left(RR\right) A d_q Q_R$$

where ϕ_0 is the stoichiometric mole fraction of the combustible mixture, *RR* is the reaction rate, *A* is a small element of area within the plate, *d* is the distance between the plates, and $\dot{Q}_R$ is the heat of reaction. In a similar manner, the rate of heat loss can be expressed by Fourier's law,

$$\dot{q}_L = kA\frac{dT}{dx}$$

where *k* is the thermal conductivity and *dT*/*dx* is the temperature gradient along the space between the two plates. Approximating the temperature distribution in the gas phase by two linear straight-line segments with a maximum temperature T_q at the center, we may equate the two previous equations and solve for the quenching distance d_q,

$$2Ak\frac{T_q - T_0}{d_q/2} = \phi_0 \dot{Q}_R \left(RR\right) A d_q$$

$$\therefore d_q = \sqrt{\frac{4k\left(T_q - T_0\right)}{\phi_0 \left(RR\right)\dot{Q}_R}} \quad \text{(I)}$$

where T_0 is the temperature at the cold boundary. Performing an energy balance, the heat of reaction may be stated as

$$\dot{Q}_R = c\left(T_f - T_0\right)$$

where *c* is the specific heat capacity at constant pressure and T_f is the flame temperature. Substituting in (I) brings to

$$\therefore d_q = \sqrt{\frac{4k}{\phi_0 c\left(RR\right)}\frac{\left(T_q - T_0\right)}{\left(T_f - T_0\right)}}$$

so that

$$\therefore d_q = \sqrt{\frac{4 \times 0.09}{1.4 \times 2.23 \times 1.2} \times \frac{\left(450 - 300\right)}{\left(2200 - 300\right)}} = 0.0871\,\text{m}$$

$$\therefore \boxed{d_q = 8.71\,\text{cm}}$$

▶ The correct answer is **C**.

P.5 ➡ *Solution*

1.True. In the ZFK framework, the normal flame velocity varies with reaction order *n* in accordance with the proportion

$$S_L \propto P^{\frac{n}{2}-1}$$

which means that, for bimolecular reactions (n = 2), the normal flame velocity is independent of pressure. The same proportion indicates that flame velocity increases with pressure for trimolecular reactions, and decreases with pressure for first-order reactions.

2.False. In the Burke-Schumann diffusion flame, diffusion in the axial direction is negligible in comparison to that in the radial direction.

3.False. The flammability range of ethane is 0.50 < Φ < 2.72. Noting that MW_F = 30 g/mol for ethane, we first compute the partial pressure

$$P_F = \frac{m_F \left(R_u / MW_F\right) T}{V_{\text{room}}} = \frac{1.0 \times \left(8315/30\right) \times 298}{\left(3.5 \times 4.5 \times 2.5\right)} = 2100\,\text{Pa}$$

The propane mole fraction is

$$\chi_F = \frac{P_F}{P} = \frac{2100}{101{,}325} = 0.0207$$

The air mole fraction is, in turn,

$$\chi_{\text{air}} = 1 - \chi_F = 1 - 0.0207 = 0.9793$$

The air-fuel ratio of the mixture in the room is

$$\left(A/F\right) = \frac{\chi_{\text{air}} MW_{\text{air}}}{\chi_F MW_F} = \frac{0.9793 \times 28.85}{0.0207 \times 30} = 45.5$$

Referring to the definition of Φ and noting that the stoichiometric air-fuel ratio for ethane is taken as 16.0, we have

$$\Phi = \frac{16.0}{45.5} = 0.352$$

This value of Φ is lower than the lean/lower flammability limit associated with ethane, which is 0.50. Accordingly, the mixture in the room is not capable of supporting a flame.

4.False. This is a simple graph-reading exercise. Entering 40 vol.% O_2 into the graph, we read an adiabatic flame temperature of 2700 K, which corresponds to about 2427 degrees Celsius.

5.True. Indeed, the graph shows that, for a given mixture pressure, increasing the volumetric content of O_2 reduces the quenching distance; this implies that oxygen enrichment tends to make flames more stable by reducing the effect of the diluent nitrogen. In general, adding inerts to the fuel or oxidant tends to make flames less stable (Baukal, Jr., 2013).

Reference: Baukal, Jr. (2013).

6.False. This is also a simple graph interpretation exercise. Drawing a vertical line from a stoichiometric ratio equal to 1 and then reading the burning velocity on the vertical axis, we get ≈2.1 m/s. Dowdy *et al.* (1990) note that the maximum burning velocity they obtained was about 2.85 m/s for a stoichiometry of 1.4 (about 41% hydrogen).

Reference: Dowdy *et al.* (1991).

7.False. The mass entrainment rate of a circular, free jet can be estimated by equation 3 in the Additional Information section,

$$\frac{\dot{m}_\infty}{\dot{m}_j} = 0.28 \left(\frac{\rho_\infty}{\rho_j}\right)^{\frac{1}{2}} \left(\frac{x}{d}\right)$$

where $\dot{m}_\infty$ is the mass of the surrounding gas entrained, $\dot{m}_j$ is the mass of the jet, ρ_∞ is the density of the surrounding gas, ρ_j is the density of the free jet, x is the distance downstream of the nozzle exit, and d is the diameter of the nozzle port. Substituting the pertaining data brings to

$$\frac{\dot{m}_\infty}{\dot{m}_j} = 0.28 \times \left(\frac{1.205}{0.668}\right)^{\frac{1}{2}} \times \left(\frac{0.20}{0.0016}\right) = \boxed{47.0}$$

8.True. Indeed, the hollow squares, which refer to the maximum flame velocity of alkanes, form a nearly horizontal line. This indicates that for alkanes of 2 to 7 carbons the maximum flame velocity is approximately the same (≈0.75 m/s).

9.True. We first estimate the density of acetylene under the conditions of interest,

$$\rho = \frac{P}{\left(R_u/MW\right)T} = \frac{101{,}325}{\left(8314/26\right)\times 340} = 0.932\,\text{kg/m}^3$$

The Reynolds number for a jet flowing at 4 cm/s is then

$$\text{Re}_{j,1} = \frac{\rho u R}{\mu} = \frac{0.932 \times 0.04 \times 0.01}{9.5 \times 10^{-5}} = 3.92$$

The corresponding spreading angle is determined to be (equation 4.1)

$$\alpha = \tan^{-1}\left(2.97/\text{Re}_{j,1}\right) = \tan^{-1}\left(2.97/3.92\right) = \boxed{37.2^\text{o}}$$

Proceeding similarly with an 20-cm/s jet, we obtain a Reynolds number $Re_{j,2}$ = 19.6 and a spreading angle such that

$$\alpha = \tan^{-1}\left(2.97/\text{Re}_{j,2}\right) = \tan^{-1}\left(2.97/19.6\right) = \boxed{8.62^\text{o}}$$

Accordingly, the slower jet is about 4.32 times wider than the faster one.

10.False. The stoichiometric fuel mass fraction is given by

$$Y_{F,\text{stoic}} = \frac{m_F}{m_A + m_F} = \frac{1}{\left(A/F\right)_\text{stoic} + 1}$$

where the stoichiometric air-fuel ratio for acetylene (x = 2, y = 2) is

$$\left(A/F\right)_\text{stoic} = \left(x + y/4\right) \times 4.76 \times \frac{MW_A}{MW_F}$$

$$\therefore \left(A/F\right)_\text{stoic} = \left(2 + 2/4\right) \times 4.76 \times \frac{28.85}{26} = 13.2$$

so that

$$Y_{F,\text{stoic}} = \frac{1}{13.2 + 1} = 0.0704$$

To find the axial location where the centerline fuel mass fraction takes on the stoichiometric value, we put $Y_{F,0} = Y_{F,\text{stoic}}$ into equation 4.2 in the Additional Information section and solve for x,

$$x = \left(\frac{0.375\,\text{Re}_j}{Y_{F,\text{stoic}}}\right) R = \left(\frac{0.375 \times 19.6}{0.0704}\right) \times 0.01 = \boxed{1.04\,\text{m}}$$

The mass fraction will reduce to the stoichiometric value at approximately one meter away from the exit.

11.False. As noted by Glassman and Yetter (2013), the laminar flame speed can be shown to scale in accordance with the Arrhenius-like proportion

$$S_L \propto \left[\exp\left(-E/R_u T_f\right)\right]^{1/2}$$

where E is activation energy, R_u is the universal gas constant, and T_f is the flame temperature. Denoting conditions before and after the diluent is added as 1 and 2, respectively, we can write the ratio

$$\frac{S_{L,2}}{S_{L,1}} = \frac{\left[\exp\left(-E/R_u T_{f,2}\right)\right]^{1/2}}{\left[\exp\left(-E/R_u T_{f,1}\right)\right]^{1/2}} = \frac{\left[\exp\left(-160,000/\left(8.314\times 1450\right)\right)\right]^{1/2}}{\left[\exp\left(-160,000/\left(8.314\times 1600\right)\right)\right]^{1/2}} = 0.537$$

so that, with $S_{L,1}$ = 30 cm/s, we obtain

$$S_{L,2} = 0.537\times S_{L,1} = 0.537\times 30 = \boxed{16.1\,\text{cm/s}}$$

Thus, decreasing the temperature from 1600 to 1450 K (a 9.4% decrease) will reduce the flame speed from 30 cm/s to 16.1 cm/s (a 46.3% decrease).

Reference: Glassman and Yetter (2015).

12.True. The equation to use is 5.1 in the Additional Information section; in the present case,

$$t_{\text{ig}} \approx \frac{\rho c \ell \left(T_{\text{ig}} - T_\infty\right)}{q_l''} = \frac{1300\times 340\times\left(1.5\times 10^{-3}\right)\times\left(573-273\right)}{30,000} = \boxed{6.63\,\text{s}}$$

The drapery will ignite within approximately 6.6 seconds.

Reference: Quintiere (2017).

13.False. Assuming the board is thick enough for the ignition time to be modelled by equation 5.2, we write

$$t_{\text{ig}} \approx \frac{\left(\pi/4\right) k\rho c\left(T_{\text{ig}} - T_\infty\right)^2}{q_l''^2} = \frac{\left(\pi/4\right)\times 0.16\times 800\times 2800\times\left(598-273\right)^2}{40,000^2} = \boxed{18.6\,\text{s}}$$

The board will ignite within approximately 19 seconds.

Reference: Quintiere (2017).

14.False. We first compute the energy release rate $\dot{Q}$, namely

$$\dot{Q} = \dot{m}'' A \Delta H_c = 55\times\left(\frac{\pi}{4}\times 1.4^2\right)\times 43.7 = 3700\,\text{kW}$$

so that, using the Heskestad formula (equation 6 in the Additional Information section),

$$L_f = 0.23\dot{Q}^{2/5} - 1.02D = 0.23\times 3700^{2/5} - 1.02\times 1.4 = \boxed{4.72\,\text{m}}$$

15.True. We can use the Heskestad formula to compute the energy release rate $\dot{Q}$, namely

$$L_f = 0.23\dot{Q}^{2/5} - 1.02D \rightarrow 3.0 = 0.23\dot{Q}^{2/5} - 1.02\times 0.8$$

$$\therefore \dot{Q} = \left(\frac{3.0 + 1.02\times 0.8}{0.23}\right)^{5/2} = 1120\,\text{kW}$$

Therefore, the mass flux $\dot{m}''$ is

$$\dot{Q} = \dot{m}'' A \Delta H_c \rightarrow \dot{m}'' = \frac{\dot{Q}}{A\times \Delta H_c}$$

$$\therefore \dot{m}'' = \frac{1120}{\left(\frac{\pi}{4}\times 0.8^2\right)\times 44.6} = \boxed{50.0\,\text{g/m}^2\cdot\text{s}}$$

16.False. We first substitute ϕ = 1.0 into the hydrogen/air flame speed correlation,

$$S_{\text{H}_2} = 0.08925 + 1.59163\times 1.0 - 0.91917\times 1.0^2 + 0.52964\times 1.0^3 = 1.29\,\text{m/s}$$

Then, we proceed similarly with the carbon monoxide/air correlation,

$$S_{\text{CO}} = 0.03276 + 0.18198\times 1.0 - 0.04156\times 1.0^2 - 0.00791\times 1.0^3 = 0.165\,\text{m/s}$$

Lastly, we substitute the foregoing results, along with x = 40%, into the equation for speed increment,

$$\frac{S_{40\%} - S_{\mathrm{CO}}}{S_{\mathrm{H_2}} - S_{\mathrm{CO}}} = -0.05914 + 0.00875x$$

$$\therefore \frac{S_{40\%} - 1.29}{1.29 - 0.165} = -0.05914 + 0.00875 \times 40 = 0.291$$

$$\therefore \boxed{S_{40\%} = 1.62\,\mathrm{m/s}}$$

Reference: Dong *et al.* (2009).

17.True. The method of Wu and Law (1985) is fairly robust and covers flame regimes for several mixture effective Lewis numbers and, with the proper adjustments, applies regardless of whether the flame is positively or negatively stretched.

Reference: Wu and Law (1985).

18.True. Specifically, Wu *et al.* (2014) found that flame speeds obtained via the extrapolation techniques they employed deviated from numerical simulation results by about 10% in the case of very lean and very rich *n*-heptane-air mixtures, while, in the case of H_2-air flames, the disagreement could be as high as 60%.

Reference: Wu *et al.* (2014).

19.False. Vagelopoulos *et al.* (1994) recommended that, for better accuracy in use of the linear interpolation technique, the Karlovitz number should be of the order of 0.1. Further, results can be improved by either reducing the strain rate or increasing the nozzle separation distance.

Reference: Vagelopoulos *et al.* (1994).

20.False. Much to the contrary, Kuznetsov *et al.* (2005) found that the run-up distance of the H_2-O_2 mixture they studied is mostly independent of tube diameter. The maximum scale of turbulent pulsations observed along the tube was found to be a much more reliable predictor of run-up distance.

Reference: Kuznetsov *et al.* (2005).

21.True. Regardless of the equivalence ratio, Tang *et al.* (2011) found that the kinetic term contributed the most to the burning flux; the sensitivity factor for the thermal effect was smaller but nevertheless still significant; lastly, the diffusional effect was the mildest of the three – indeed, the linearity between burning flux and the hydrogen addition parameter was barely affected when the variation in the Lewis number *Le* was suppressed altogether.

Reference: Tang *et al.* (2011).

22.True. In Blint's (1986) model, the flame width δ_T, which stems from a temperature gradient definition, was found to correlate well with the transport properties of the burned gases. The flame width δ_τ, which is based on a characteristic chemical time, was found to correlate with the transport properties of the unburned gases. Lastly, the flame width δ_Q, which is related to the half-width of the heat release rate, did not correlate with any reasonable transport property of the gases.

Reference: Blint (1986).

23.True. Indeed, Buckmaster *et al.* (1990) noted that for Lewis numbers not too small, flame balls are much more tenacious than plane flames. At *Le* = 0.3, which is representative of lean H_2-air mixtures, flame balls may exist in the presence of heat losses nearly 300 times stronger than those required to extinguish plane flames.

Reference: Buckmaster *et al.* (1990).

24.False. Much to the contrary, Smooke *et al.* (1989) used a two-dimensional geometry discretized by a finite-difference scheme. Since it relied on stream functions, Smooke's model cannot be readily converted to a three-dimensional framework.

Reference: Smooke *et al.* (1989).

25.False. An ABB double cone burner exhibits a central recirculation zone containing hot combustion products downstream of the burner exit, which acts as a hydrodynamic flame holder. Zimont *et al.* (1998) note that their model exhibited significant discrepancies with respect to the size and location of the central recirculation zone, which in the model was predicted to be exceedingly wide and long. The strength of the recirculation was also significantly overpredicted.

Reference: Zimont *et al.* (1998).

26.False. In Barlow and Frank's experiments, increasing turbulence was associated with significantly greater peak mass fractions of OH, H_2 and NO, modestly greater peak mass fractions of H_2O and CO, and decreased peak mass fractions of CO_2.

Reference: Barlow and Frank (1998).

27.False. The results by Hawkes and Cant (2000) were actually encouraging. Their plots of flame density showed an increase in flame thickness and a decrease of resolved wrinkling with increased Δ, just as one would expect from a LES-FSD model. The integrated consumption rate (i.e., the product of flame surface density and laminar consumption rate) remained approximately constant under variations of Δ. Hawkes and his colleague followed up with further research on the implications of varying filter widths Δ on the feasibility of LES-FSD simulations; see, for instance, Hawkes and Cant (2001).

References: Hawkes and Cant (2000); Hawkes and Cant (2001).

28.False. This is yet another little observational exercise: inspection of the plot shows that the three curvature PDFs for the slot flame produced by Bell's team showed very similar results, which is surprising in view of the fact that Ashurst and Shepherd (1997) had suggested that 2D curvature computations were prone to overestimate the 3D values.

References: Bell *et al.* (2007); Ashurst and Shepherd (1997).

29.True. Yoo *et al.* (2009) noted that large values of Damköhler number near the flame base, the existence of HO_2 upstream of high-temperature radicals (O, OH and H) and the balance of two specific reactions,

$$\mathrm{HO_2 + H \rightarrow OH + OH}$$

$$\mathrm{H + O_2 + M \rightarrow HO_2 + M}$$

at the flame base are all hallmarks of auto-ignition.

Reference: Yoo *et al.* (2009).

30.False. In actuality, Gruber *et al.* (2010) found a flame thickness behavior opposite to the one described in the statement; that is, the flame thickness at the centerline was close to the laminar flame thickness, while close to the wall there was a considerable thickening of the flame. The result is a 'combustion regime change' from a thin flamelet regime near the channel centerline to a thickened wrinkled regime close to the wall.

Reference: Gruber *et al.* (2010).

31.True. Floyd *et al.* (2009) summarize some of the shortcomings of the β-function, including its fragile theoretical basis, its inability to reliably represent bimodal behavior for some conserved scalars, and its limited capacity to represent some states found in non-binary shear layers and jets.

References: Floyd *et al.* (2009); Tong *et al.* (2001).

32.True. The final part of the statement draws from Wu *et al.* (2003). Working with duct-like combustor geometries, Wu's team developed a comprehensive analysis of flames under acoustic perturbation and found that, at sufficiently high amplitude, such disturbances may restabilize Darrieus-Landau instability and may even control the mean shape of a flame: a conic flame may transform into a hemispherical flame as the pressure is increased.

Reference: Wu *et al.* (2003).

33.False. By inspection, we see that the large-scale flame is clearly subject to greater wrinkling. Lapenna *et al.* (2018) note that large-scale flames, when compared to small-scale flames under similarly weak turbulent conditions, are characterized by overall larger wrinkling factors.

Reference: Lapenna *et al.* (2019).

34.False. In their paper, Brisley *et al.* (2005) indeed note that the lack of rotational symmetry in turbulent burner flames may hinder use of their imaging technique, but they note that a turbulent flame, when averaged over a period of time, will also exhibit significant rotational symmetry, allowing the same reconstruction algorithm to be applied even though the reconstructions are only achieved over the averaged cross-sections of the flame.

Reference: Brisley *et al.* (2005).

35.True. Indeed, Chaudhuri *et al.* (2012) proposed that a "turbulent Reynolds number" such that

$$\mathrm{Re}_{T,\langle R\rangle} = \left(\frac{u_{\mathrm{rms}}}{S_L}\right)\left(\frac{\langle R\rangle}{\delta_L}\right)$$

where u_{rms} is the root-mean-square velocity, S_L is the flame speed, δ_L is the flame thickness, and $\langle R\rangle = \sqrt{A/\pi}$, where A is the area enclosed by the spherical flame edge tracked by their camera apparatus. Chaudhuri's team found that the entirety of the flame propagation rate data were well-represented by a power law with $Re_{T,\langle R\rangle}$ taken to the 0.54 power, in reasonable agreement with a 1/2-power theoretical scaling that Chaudhuri and his collaborators had proposed in an earlier paper.

Reference: Chaudhuri *et al.* (2012).

36.False. As shown below, van den Boom obtained an exponential relationship between the product $E_x \times x$ (where E_x is the electric field strength in the pre-flame zone and x is the position of the flame front or stand-off distance) and the velocity deviation ΔS_L; the solid line is the exponential fit ΔS_L [cm/s] = $0.014exp(E_x x$ [kV]) and the data points refer to different heights of the upper electrode used in their experimental arrangement.

Reference: Van den Boom *et al.* (2009).

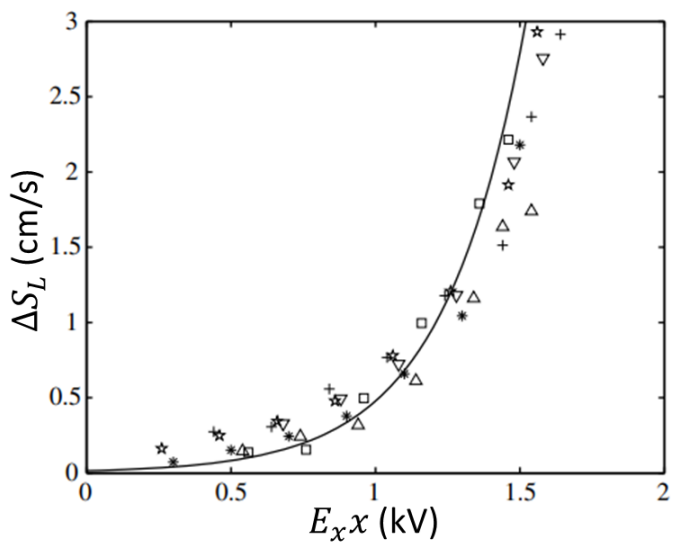

37.False. Much to the contrary, Bar-Ilan *et al.* (2004) found that to achieve a smolder velocity of 0.10 mm/s with forced flow, the microgravity total oxidizer mass flux is 0.30 g/m^2·s, whereas the normal-gravity forced-flow test total oxidizer mass flux was calculated to be around 0.60 g/m^2·s. In a similar manner, the smolder velocity in microgravity at an oxidizer mass flux of 0.58 g/m^2·s is the same as that of a normal-gravity forced flow with an oxidizer mass flux around 0.85 g/m^2·s. These observations suggest that the presence of buoyant heat losses in normal gravity hinders the smolder reaction and that a significantly higher oxidizer mass flux is required to obtain the same smolder propagation velocity as in microgravitational conditions.

Reference: Bar-Ilan *et al.* (2004).

38.False. In actuality, Chen's team observed that oscillatory coupling between two flames varied from in-phase behavior at short distances, anti-phase behavior at intermediate distances, and incoherent behavior at long distances.

Reference: Chen *et al.* (2019).

P.6 ➡ *Solution*

Alternative E contains the correct associations. See Lipatnikov and Chomiak (2002) for the corresponding references.

▶ The correct answer is **E**.

P.7 ➡ *Solution*

We first compute the Reynolds number,

$$\mathrm{Re} = \frac{Ud}{\nu} = \frac{10\times 0.125}{1.5\times 10^{-5}} = 83{,}300$$

This is much greater than the $Re \approx 2000$ threshold for turbulent internal flows, so we surmise that the flame is turbulent. To estimate the turbulent flame speed, we require the turbulent dissipation rate. To estimate

the dissipation rate, in turn, we may consider the work done by pressure drop in the pipe flow; the work w per unit mass associated with a pressure drop Δp is

$$w = -\frac{1}{\rho}\Delta p \quad \text{(I)}$$

The pressure drop is given by the Darcy-Weisbach equation,

$$\Delta p = -f_F \frac{L}{d}\frac{\rho U^2}{2}$$

where f_F is the Fanning friction factor and L is the length of the pipe. To obtain the total power Π dissipated in the length L, we multiply (I) by the mass flow rate $\dot{m}$, that is,

$$\Pi = -\frac{1}{\rho}\Delta p \times \underbrace{\frac{\pi}{4}d^2 \rho U}_{=\dot{m}}$$

$$\therefore \Pi = -\frac{\pi}{4}\Delta p d^2 U = -\frac{\pi}{4}\times\left(-f_F \frac{L}{d}\frac{\rho U^2}{2}\right)\times d^2 U$$

$$\therefore \Pi = f_F \frac{\pi}{8}\rho d L U^3$$

The turbulent dissipation rate is the energy dissipation per unit mass, which we find by dividing Π by the total mass of fuel contained in the length L,

$$\varepsilon = \frac{\Pi}{\dot{m}} = \frac{f_F \frac{\pi}{8}\rho d L U^3}{\frac{\pi}{4}\rho d^2 L} = f_F \frac{1}{2}\frac{U^3}{d}$$

The Fanning friction factor for a turbulent flow such that $2100 < Re_d < 100{,}000$ can be determined as

$$f_F = \frac{0.0791}{\mathrm{Re}^{1/4}} = \frac{0.0791}{83{,}300^{1/4}} = 0.00466$$

so that

$$\varepsilon = f_F \frac{1}{2}\frac{U^3}{d} = 0.00466 \times \frac{1}{2} \times \frac{10^3}{0.125} = 18.6\,\mathrm{m^2\,s^{-3}}$$

Now, ε is related to the characteristic velocity fluctuation u' by an expression of the form

$$\varepsilon = \frac{A u'^3}{d}$$

where A is a constant of order unity. Assuming $A \approx 1$, we solve for u' to obtain

$$u' = (\varepsilon d)^{1/3} = (18.6 \times 0.125)^{1/3} = 1.32\,\mathrm{m/s}$$

The Taylor microscale λ is, in turn,

$$\lambda = d\left(\frac{15}{A \times \mathrm{Re}}\right)^{1/2} = 0.125 \times \left(\frac{15}{1.0 \times 83{,}300}\right)^{1/2} = 0.00168\,\mathrm{m}$$

The Kolmogorov microscale, in turn, is

$$\eta = \left(\frac{\nu^3}{\varepsilon}\right)^{1/4} = \left[\frac{\left(1.5 \times 10^{-5}\right)^3}{18.6}\right]^{1/4} = 0.000116\,\mathrm{m}$$

Note that the Taylor microscale is considerably larger than the Kolmogorov microscale. Now, the turbulent flame spreads at a velocity S_T such that

$$S_T = S_L + u'$$

where S_L = 0.38 m/s is the laminar speed under analogous conditions. Thus,

$$S_T = 0.38 + 1.32 = \boxed{1.70\,\text{m/s}}$$

It remains to compute the flame thickness δ_F, which, using the Taylor microscale as a characteristic length, becomes

$$\delta_F = \frac{u'\lambda_c}{S_L} \approx \frac{u'\lambda}{S_L} = \frac{1.32 \times 0.00168}{0.38} = 0.00584\,\text{m}$$

$$\therefore \boxed{\delta_F = 5.84\,\text{mm}}$$

The turbulent flame has a velocity of 1.70 m/s and a thickness of approximately 5.8 millimeters.

▶ The correct answer is **C**.

REFERENCES

- Ashurst, W.T. and Shepherd, I.G. (1997). Flame front curvature distributions in a turbulent premixed flame zone. *Combust Sci Technol*, 124(1-6), 115 – 144.
- Bar-Ilan, A., Rein, G., Walther, C. *et al.* (2004). The effect of buoyancy on opposed smoldering. *Combust Sci Technol*, 176(12), 2027 – 2055.
- Barlow, R.S. and Frank, J.H. (1998). Effects of turbulence on species mass fractions in methane/air jet flames. *Symp (Int) Combust*, 27(1), 1087 – 1095.
- BAUKAL JR., C.E. (2013). *Oxygen-Enhanced Combustion.* 2nd edition. Boca Raton: CRC Press.
- Bell, J.B., Day, M.S., Grcar, J.F. *et al.* (2007). Numerical simulation of a laboratory-scale turbulent slot flame. *Proc Combust Inst*, 31(1), 1299 – 1307.
- Blint, R.J. (1986). The relationship of the laminar flame width to flame speed. *Combust Sci Technol*, 49(1-2), 79 – 92.
- Brisley, P.M. (2005). Three-dimensional temperature measurement of combustion flames using a single monochromatic CCD camera. *IEEE Trans Instrum Meas*, 54(4), 1417 – 1421.
- Buckmaster, J., Joulin, G. and Ronney, P. (1990). The structure and stability of nonadiabatic flame balls. *Combust Flame*, 79, 381 – 392.
- Chaudhuri, S., Wu, F., Zhu, D. *et al.* (2012). Flame speed and self-similar propagation of expanding turbulent premixed flames. *Phys Rev Lett*, 108, 044503.
- Chen, T., Guo, X., Jia, J. *et al.* (2019). Frequency and phase characteristics of candle flame oscillation. *Sci Rep*, 342(9).
- Dong, C., Zhou, Q., Zhao, Q. *et al.* (2009). Experimental study on the laminar flame speed of hydrogen/carbon monoxide/air mixtures. *Fuel*, 88(10), 1858 – 1863.
- Dowdy, D.R., Smith, D.B. and Taylor, S.C. (1991). The use of expanding spherical flames to determine burning velocities and stretch effects in hydrogen/air mixtures. *Symp (Int) Combust*, 23(1), 325 – 332.
- FLAGAN, R.C. and SEINFELD, J.H. (1988). *Fundamentals of Air Pollution Engineering*. Engelwood Cliffs: Prentice Hall.
- Floyd, J., Kempf, A.M., Kronenburg, A. *et al.* (2009). A simple model for the filtered density function for passive scalar combustion LES. *Combust Theory Model*, 13(4), 559 – 588.
- GLASSMAN, I., YETTER, R.A. and GLUMAC, N.G. (2015). *Combustion.* 5th edition. London: Academic Press.
- Gruber, A., Sankaran, R., Hawkes, E.R. *et al.* (2010). Turbulent flame-wall interaction: a direct numerical simulation study. *J Fluid Mech*, 658, 5 – 32.
- Hawkes, E.R. and Cant, R.S. (2000). A flame surface density approach to large-eddy simulation of premixed turbulent combustion. *Proc Combust Inst*, 28(1), 51 – 58.
- Hawkes, E.R. and Cant, R.S. (2001). Physical and numerical realizability requirements for flame surface density approaches to large-eddy and Reynolds averaged simulation of premixed turbulent combustion. *Combust Theory Model*, 5(4), 699 – 720.
- Kelley, A.P. and Law, C .K. (2009). Nonlinear effects in the extraction of laminar flame speeds from expanding spherical flames. *Combust Flame*, 156(9), 1844 – 1851.
- Kuznetsov, M., Alekseev, V., Matsukov, I. *et al.* (2005). DDT in a smooth tube filled with a hydrogen-oxygen mixture. *Shock Waves*, 14(3), 205 – 215.
- Lapenna, P.E., Lamioni, R., Troiani, G. *et al.* (2019). Large scale effects in weakly turbulent premixed flames. *Proc Combust Inst*, 37(2), 1945 – 1952.

- Lipatnikov, A.N. and Chomiak, J. (2002). Turbulent flame speed and thickness: phenomenology, evaluation, and application in multi-dimensional simulations. *Prog Energy Combust Sci*, 28, 1 – 74.
- MUKHOPADHYAY, A. and SEN, S. (2019). *Fundamentals of Combustion Engineering*. Boca Raton: CRC Press.
- QUINTIERE, J.G. (2017). *Principles of Fire Behavior*. 2nd edition. Boca Raton: CRC Press.
- Searby, G. and Rochwerger, D. (1991). A parametric acoustic instability in premixed flames. *J Fluid Mech*, 231, 529 – 543.
- Smooke, M.D., Mitchell, R.E. and Keyes, D.E. (1989). Numerical solution of two-dimensional axisymmetric laminar diffusion flames. *Combust Sci Tech*, 67(4-6), 85 – 122.
- Tang, C.L., Huang, Z.H. and Law, C.K. (2011). Determination, correlation, and mechanistic interpretation of effects of hydrogen addition on laminar flame speeds of hydrocarbon-air mixtures. *Proc Combust Inst*, 33(1), 921 – 928.
- Tong, C. (2001). Measurements of conserved scalar filtered density function in a turbulent jet. *Phys Fluids*, 13(10), 2923 – 2937.
- TURNS, S.R. (2012). *An Introduction to Combustion*. 3rd edition. New York: McGraw-Hill.
- Vagelopoulos, C.M., Egolfopoulos, F.N. and Law, C.K. (1994). Further considerations on the determination of laminar flame speeds, *Symp (Int) Combust*, 25(1), 1341 – 1347.
- Van den Boom, J.D.B.J., Konnov, A.A., Verhasselt, A.M.H.H. *et al.* (2009). The effect of a DC electric field on the laminar burning velocity of premixed methane/air flames. *Proc Combust Inst*, 32(1), 1237 – 1244.
- Wu, C.K. and Law, C.K. (1985). On the determination of laminar flame speeds from stretched flames. *Symp (Int) Combust*, 20(1), 1941 – 1949.
- Wu, F., Liang, W., Chen, Z. *et al.* (2014). Uncertainty in stretch extrapolation of laminar flame speed from expanding spherical flames. *Proc Combust Inst*, 35(1), 663 – 670.
- Wu, X., Wang, M., Moin, P. *et al.* (2003). Combustion instability due to the nonlinear interaction between sound and flame. *J Fluid Mech*, 497, 23 – 53.
- Yoo, C.S., Sankaran, R. and Chen, J.H. (2009). Three-dimensional direct numerical simulation of a turbulent lifted hydrogen jet flame in heated coflow: flame stabilization and structure. *J Fluid Mech*, 640, 453 – 481.
- Yu, G., Law, C.K. and Wu, C.K. (1986). Laminar flame speeds of hydrocarbon + air mixtures with hydrogen addition. *Combust Flame*, 63, 339 – 347.
- Zimont, V., Polifke, W., Bettelini, M. *et al.* (1998). An efficient computational model for premixed turbulent combustion at high Reynolds numbers based on a turbulent flame speed closure. *J Eng Gas Turbines Power*, 120(3), 526 – 532.